Indian Journal of Marine Sciences
Vol. 39 (3), September 2010, pp 313-322

Spatio-temporal dynamics of suspended sediment concentration during the 2004 Sumatra tsunami

XinFeng Zhang[1,2], DanLing Tang[2], ZiZhen Li[3] & XiaoJie Dai[1]

[1]College of Marine Sciences, Key Laboratory of Sustainable Exploitation of Oceanic Fisheries Resources under Ministry of Education, Shanghai Ocean University, 999 Hucheng Huan Road, Lingang Xincheng, Shanghai, China, 201 306

[2]Center for Remote Sensing and Marine Ecology/Environment (RSMEE) and LED, South China Sea Institute of Oceanology, Chinese Academy of Sciences, West Road 164 of Xingang, Guangzhou, China, 510 301.

[3]Institute of Bioinformatics, School of Mathematics and Statistics, Lanzhou University, Lanzhou, China, 730 000

[E-mail: lingzistdl@126.com (D.L. Tang); xinfeng566@163.com (X.F. Zhang)]

Received 15 April 2009; revised 2 November 2009

Spatio-temporal dynamics of suspended sediment concentration (SSC) in Indian Ocean during the 2004 Sumatra tsunami was analyzed using satellite data. Surface SSC in epicenter area increased notably right after the tsunami week (about 200% higher than that in the same period in earlier 4 years); the surface SSC in a deep water area about 1600 km from the epicenter area did not increase after the tsunami. Increase of SSC in the epicenter area may be mainly caused by the transportation of SSC by the tsunami backwash. Range of spatial clustering in SSC significantly decreased during the tsunami week. It may be related to the tsunami waves that diluted the spatial clustering level in SSC. A new spatio-temporal correlation model shows that the fluctuation in the spatio-temporal correlation surface of SSC appeared remarkably intense round the tsunami. Present study reveals that the tsunami considerably disturbed the spatio-temporal dynamics in SSC.

[**Key words**: Indian Ocean, tsunami, suspended sediment concentration, spatio-temporal correlation, spatio-temporal model]

Introduction

Earthquake on 26 December 2004 with the epicenter off the west coast of northern Sumatra produced a great tsunami. It swept through the Indian Ocean region and caused massive damages to the marine and terrestrial environment along the coastal area[1-5]. In particular, the tsunami backwash transported lots of suspended sediment matter from the coastal land to the sea, which is very important to the marine environment since the subsequent dispersal transports many contaminants to the oceans and affects the coastal seas[6-8]. Suspended sediment concentration (SSC) can be affected in many ways. Storm surge can increase SSC and offshore transport in the estuary[9,10]. Natural physical processes (such as tidal currents, wind waves and mixing with clear ocean water) explain some of the spatial variability of SSC and associated contaminant concentrations[11-13]. In addition, phytoplankton bloom also affects SSC[14]. Floods are believed to be the fundamental events in the transfer of sediments and contaminants from the mainland to the coastal zones, and also from the coastal zones to the seas[15]. Huge suspended sediments, transported by the tsunami backwashing floods, may have polluted the Indian Ocean to a certain extent, and may have affected also the spatial distribution dynamics of SSC in the ocean surface.

Satellite-measured remote sensing has been used to infer the distribution of SSC in sea surface waters[16-17]. A few studies have been concentrated on the changes of SSC during the 2004 Sumatra tsunami. Analysis of the satellite OCM (Ocean Color Monitor) data showed considerable increase of SSC along the Andhra and Tamilnadu Coasts of India after the tsunami[18]. Satellite MODIS-aqua data showed SSC increased markedly in the estuaries of some large rivers 4 weeks after the tsunami[8]. By modeling the satellite SeaWiFS water-leaving radiance data, Zhang *et al.*[19] found that the effects of wind and rainfall on SSC weakened around the tsunami event and the changes in SSC were not significant immediately after the tsunami compared with earlier years.

Because of the flow of seawater and many other reasons (such as offshore distance, wind and rainfall), the values of SSC at two neighboring regions may not be independent. It tend to be similar, i.e., the distribution of SSC may be clustered or correlated spatially. Quantifying the degree of spatial clustering is a central issue in spatial analysis. In this study, based on a spatial correlation model developed by Lee[20], proposed a three-dimensional and spatio-temporal correlation model. An important feature of our new model is that: it accounts for the effect of time lag on the spatial correlation in SSC distribution. It gives a novel insight into the spatio-temporal dynamics of SSC distribution simultaneously along space and time. Present study consists the spatial and temporal characteristics of the distribution dynamics in SSC by using satellite data and new spatio-temporal correlation models.

Materials and Methods

Study area and satellite data

The study area is located in 5°S- 1°N × 74°E- 8°E in the eastern Indian Ocean (Fig. 1). It covers the earthquake epicenter and was most strongly influenced by the tsunami. In order to compare the changes of SSC between the epicenter area (Box E in Figure 1, 1°×1° square centered the epicenter) and two deep areas of the ocean surface far away from the epicenter and the coastal zone, we sampled two 2°×2° square areas located in 1°S-1°N × 90°E-92° and 5°S-3°S × 82°E-84°E about 650km and 1600km away from the epicenter (Boxes Q and S in Figure 1), respectively.

The satellite SeaWiFS normalized water-leaving radiance (NWR) value at 555nm (nLw 555) was related closely to the total SSC, and NWR has been used widely as a surrogate for SSC to investigate the SSC distribution dynamics[8,18,21,22]. In this study, NWR is used as a measure of surrogate for SSC and refer to NWR as SSC.

The data of NWR, 0.5° resolution at 555nm 8-day (Level 3), observed from satellite SeaWiFS, were obtained from the Ocean Color Time Series Project (http://reason.gsfc.nasa.gov/Giovanni/). Eight temporal periods (called "week" hereafter) were chosen (Fig. 2). This is done for 3 weeks before the tsunami week and 4 weeks after. In order to investigate the spatio-temporal dynamics of SSC, the SSC data in another 6 weeks, immediately before the 8 weeks, were analyzed later. The data of wind, 0.25° resolution (Level 3), observed from satellite QuickScat, were obtained from the Jet Propulsion Laboratory (http://poet.jpl.nasa.gov/).

Modeling

To solve the problem of spatial autocorrelation in a single variable *y*, Whittle[23] first proposed the famous SAR model and the standard formula as:

$$y = \rho W y + \varepsilon \qquad \ldots (1)$$

Where ρ is the coefficient of spatial dependence in variable *y*, W is *n* by *n* spatial weight matrix, Wy is the space-lagged (SL) vector of *y*. ε is the error term with normal distribution. The row-standardized spatial weight matrix W is determined by the spatial configuration of the *n* locations as:

$$W_{ij} = C_{ij} \Big/ \sum_{j=1}^{j=n} C_{ij} \quad , \; i, j = 1, \ldots, n \qquad \ldots (2)$$

Where C_{ij} = 1 if locations (or grids) *i* and *j* are immediate vertical and horizontal neighbors and 0 otherwise.

By examining the degree of ordinary Pearson correlation between a variable *x* and its SL vector *Wx*, Lee[20] proposed a spatial correlation statistic to measure the degree of spatial autocorrelation in *x*. The standard version is as:

$$r_I = z'\tilde{z} \Big/ \left(\sqrt{z'z} \sqrt{\tilde{z}'\tilde{z}} \right), \; z_i = x_i - \bar{x} \; ; \; \tilde{z}_i = \tilde{x}_i - \bar{\tilde{x}} \; ; \; \tilde{x} = Wx \; ; \; i = 1, \ldots, n \quad \ldots (3)$$

Where the transpose of z is z', $\bar{x}$ is the mean of *x*. In this study, the vector *x* is the observations of SSC at the *n* locations (or grids) in the study area (Fig. 1). Formula (3) can be used to plot spatial correlograms if the high-order spatial weight matrix W_g, g = 1, 2 ... is used. *g* is the number of spatial lags, and W_g can be derived from mathematical recursion in equation (2). Model (3) indicates the total level of spatial clustering in SSC distribution as this correlation function measures directly the correlation degree of the observations of SSC and its SL vector. The distance of spatial lag *g* may be used as a relative indicator of the size or range of spatial clustering in SSC.

It may be reasonable to consider the effect of time lag in formula (3), i.e., observation x_i at time *t* is not only correlated to the observations round the i^{th} location at time *t*, but also affected by the observations round the i^{th} location at a past time *t - k*. Then, formula (3) may be improved as:

$$r^t{}_I = z_t'\tilde{z}_{t\text{-}k} \Big/ \left(\sqrt{z_t'z_t} \sqrt{\tilde{z}_{t\text{-}k}'\tilde{z}_{t\text{-}k}} \right), \qquad \ldots (4)$$

$$z_{t_i} = x_{t_i} - \bar{x}_t \; ; \; \tilde{z}_{(t\text{-}k)_i} = \tilde{x}_{(t\text{-}k)_i} - \bar{\tilde{x}}_{(t\text{-}k)} \; ; \; \tilde{x}_{(t\text{-}k)} = W_g x_{(t\text{-}k)} \; ;$$
$$i = 1, \ldots, n \; ; \; g = 1, 2 \ldots ; \; k = 1, 2 \ldots$$

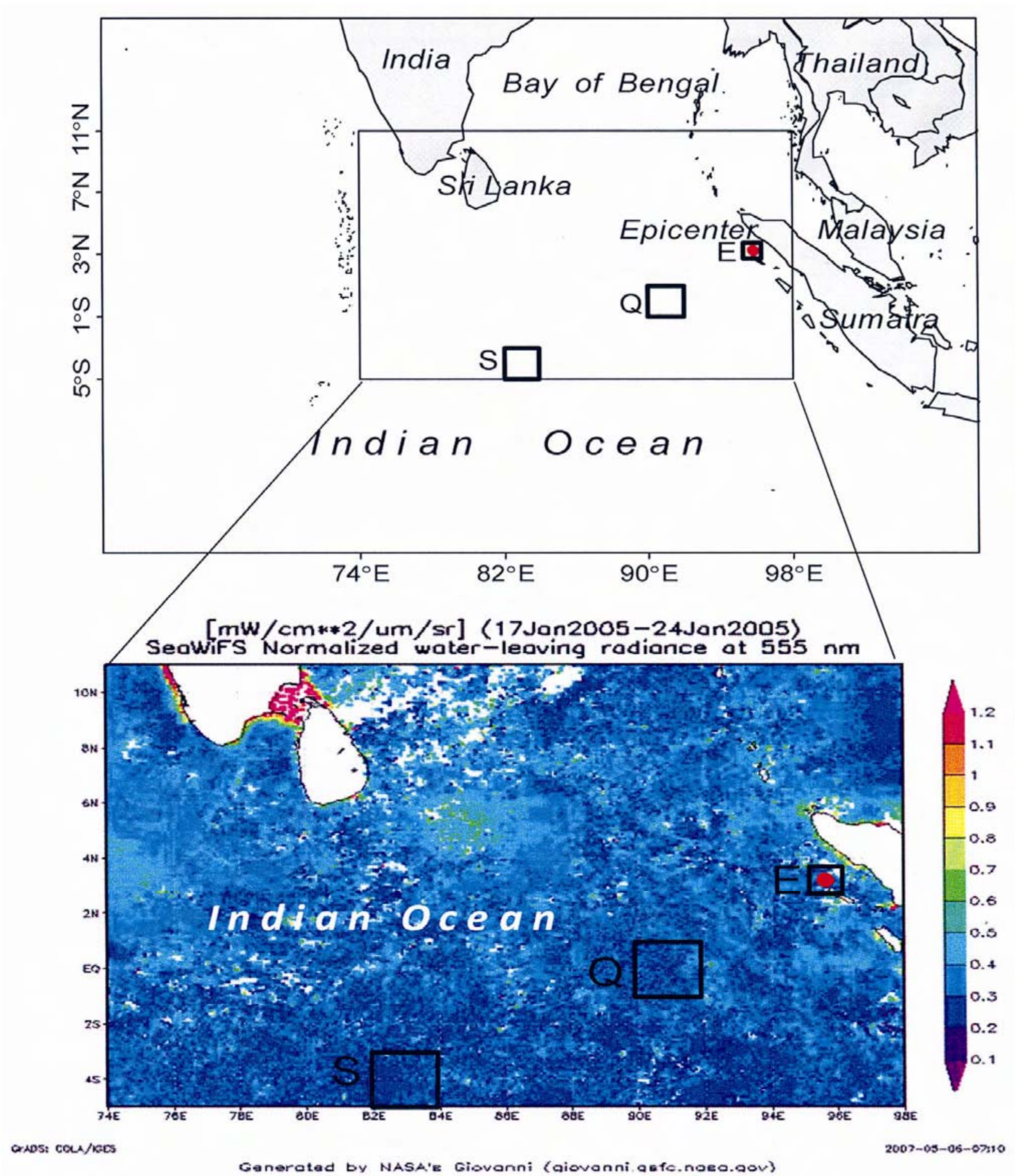

Fig. 1—SSC distribution in one week in study area (5°S-11°N × 74°E-98°E). Box E: a sampling area (1°×1° square centered the epicenter). Boxes Q and S: two sampled areas in the sea surface (2°×2° square about 650km and 1600km away from the epicenter, respectively).

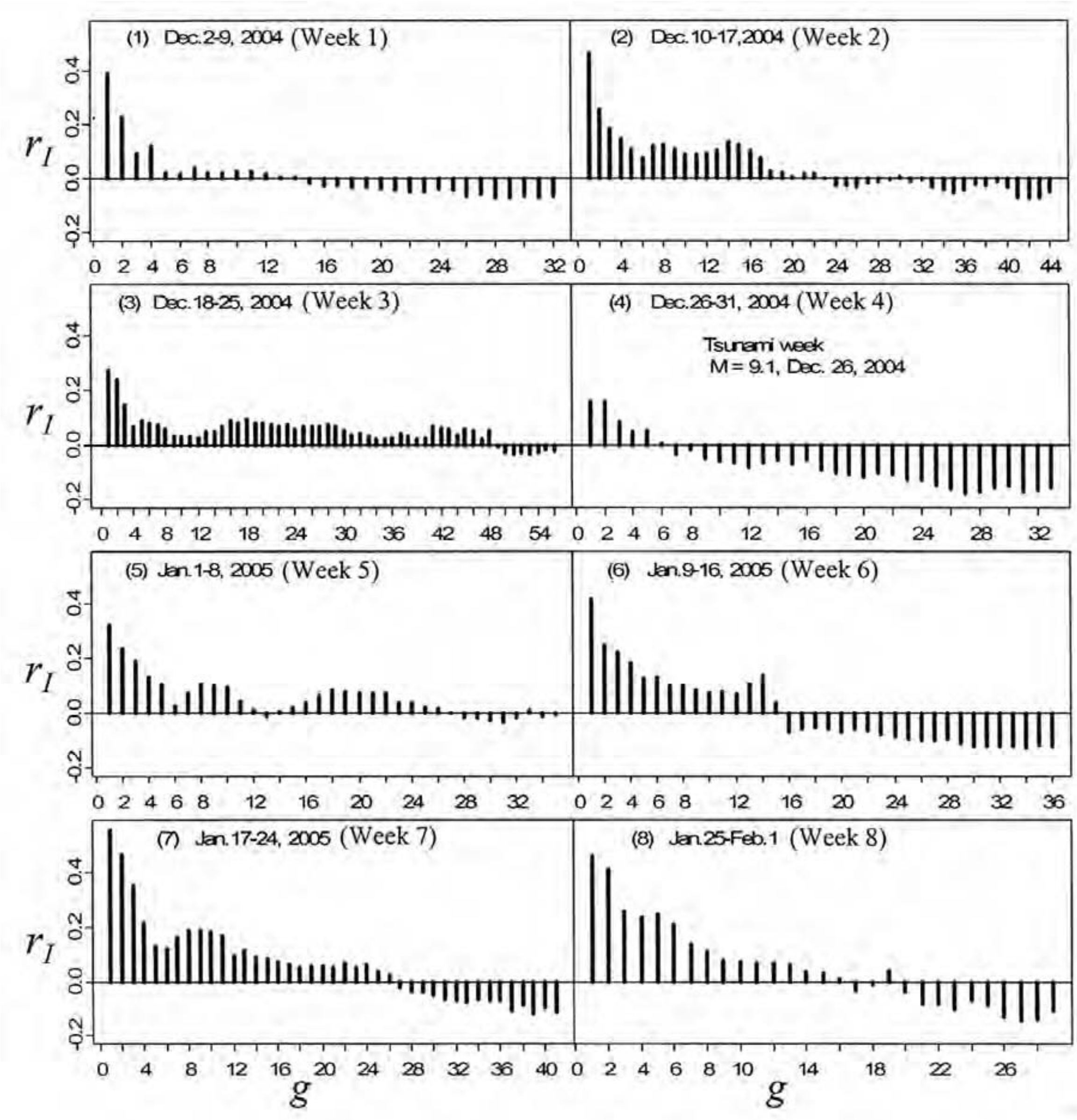

Fig. 2—Spatial correlograms for SSC along spatial lags. One spatial lag is 0.5°. r_I is the spatial autocorrelation coefficient of SSC, g is the number of spatial lags in model 3.

Where t - k (k = 1, 2 ...) is the number of time lags, x_t and $x_{(t-k)}$ are two observation vectors of the same variable x at time t and at time t - k, respectively.

Above model had been applied to model the spatio-temporal dynamics of SSC distribution. The test method in Tables 1, 2 is t test. All the above computation and test estimation were implemented using statistical software R (http://www.r-project.org).

Results

General trend in SSC from the epicenter

The SSC showed a drastic fluctuation in the epicenter area (Box E in Fig. 1) and had a significant increase and reached the maximum in Week 5 (Fig. 3 (1) a). The SSC showed a less notable fluctuation in the sampled area of Box Q (about 650km away from the epicenter) and increased noticeably two weeks after the tsunami (Fig. 3 (1) b). But SSC in the sampled deep area of the sea (Box S in Fig. 1) did not show significant changes (Fig. 3 (1) c). Comparisons of SSC in the epicenter area (Box E) in Week 5, with the same period in 4 earlier successive years, indicated that SSC was considerably higher (about 200%) than that in the same period of Jan. 1 - 8 in 4 earlier successive years (Figure 3 (2)).

Spatial distribution of SSC

The Pearson's correlation test of r_I value, calculated by formula (3), showed that SSC had significant spatial autocorrelation for each week (Table 1). But the degree of spatial correlation in SSC decreased noticeably round the tsunami occurrence. The smallest r_I value (0.16) appeared in Week 4. The high-order spatial correlograms of SSC showed that the degree of autocorrelation decreased gradually as spatial lags increased for all the 8 weeks (Fig. 2). Distance of positive correlation varied considerably among the weeks from 5 lags to 48 lags. The longest correlation distance (g = 48), which exceeded significantly the correlation distance in other weeks, appeared in Week 3 (Figure 2(3)). The smallest correlation length 5 appeared in Week 4 (Fig. 2(4)). Correlograms of Week 1 and Week 8 were generally similar and decrease consistently. This can be considered the "normal" correlograms. In order to understand the anomalous increase of spatial correlation distance in SSC immediately before the tsunami, we undertook time series comparison of spatial correlograms of SSC in Week 3 with the same period in other 5 years. The results showed that the positive correlation distance in SSC in Week 3 was significantly longer than that in the same period of Dec. 19 - 26 in other 5 years from 2001 to 2006 (Fig. 4(4)).

Table 1—Pearson correlation coefficient (r_I) test between SSC and its SL vector, and wind speed (m/s). Weeks 1, 2, 8 are in the order of the 8 weeks shown in Figure 2.

Week	1	2	3	4	5	6	7	8
r_I (SSC and its SL)	0.39	0.46	0.27	0.16	0.32	0.42	0.56	0.46
Average wind speed(m/s)	4.65	4.10	4.88	4.86	6.02	5.59	3.70	3.78

p-value < 0.0001

Spatial and temporal dynamics of SSC distribution

The temporal correlations in SSC, between the 8 weeks, were measured by formula (4) as spatial lag g = 1 (Table 2). There was a general trend of decrease in correlation over time (along each row of Table 2), this pattern was not consistent. It was noticeable that except Week 6 the significance of the temporal correlation in SSC disappeared between Week 5, 7, 8 and Week 4 (column of Week 4 in Table 2).The high-order Spatio-temporal correlograms were measured by formula (4) (Fig. 5). There is a general trend of decrease, in the spatio-temporal

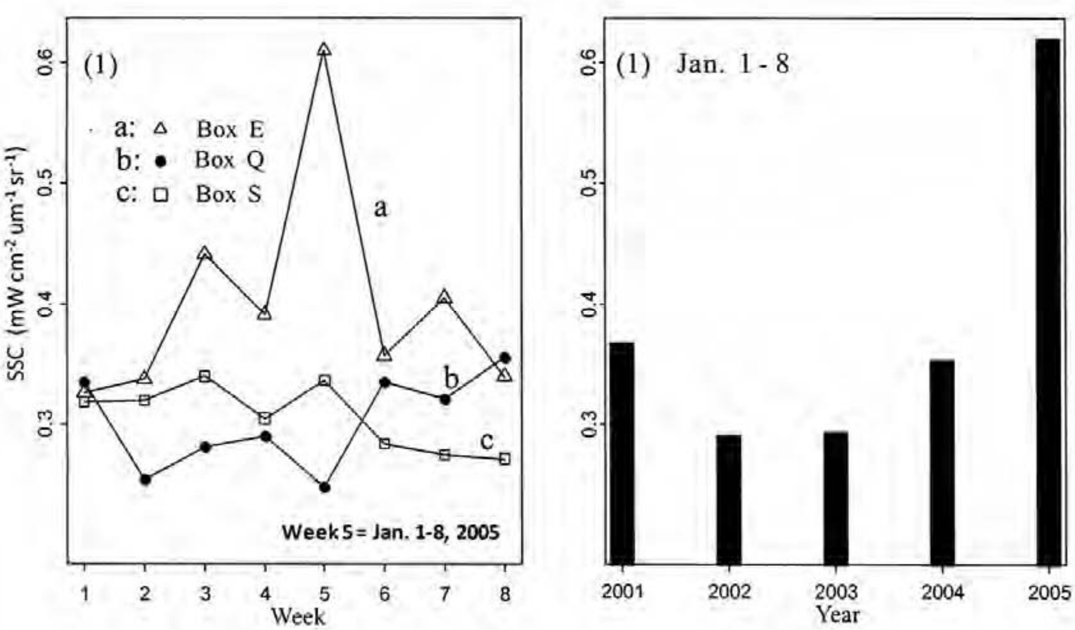

Fig. 3 (1)—. SSC content (mWcm^{-2}um^{-1}sr^{-1}) in Box E (1°×1° square centered the epicenter), in Box Q and in Box S (2°×2° squares about 650km and 1600km away from the epicenter, respectively). Weeks 1, 2 … 8 are in the order of the 8 weeks shown in Figure 2. (2). Time series for SSC in Jan. 1 – 8 from 2001 to 2005.

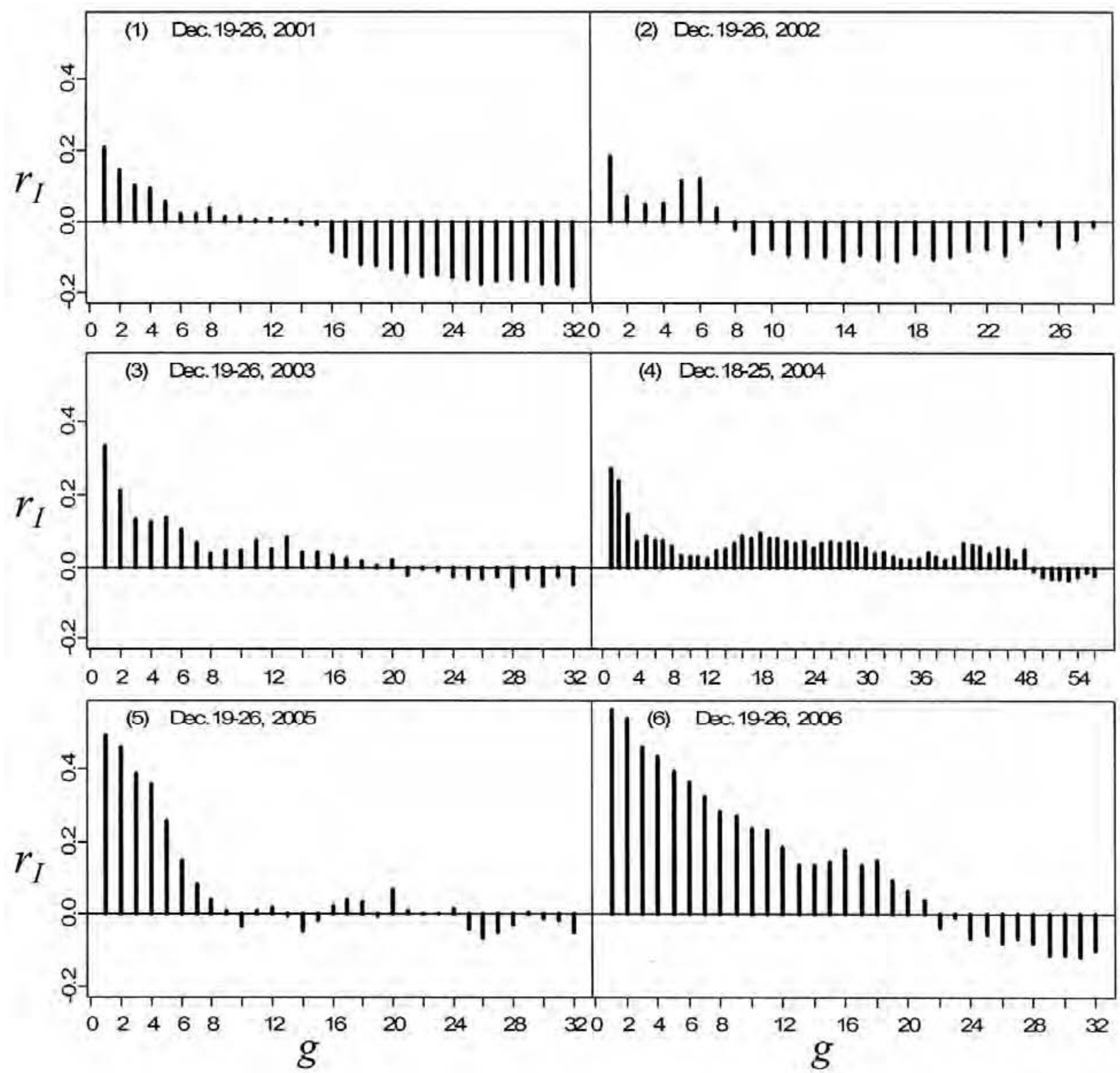

Fig. 4—Time series comparison of spatial correlograms in SSC for the week of December 18 - 25. One spatial lag is 0.5°. r_I is the spatial autocorrelation coefficient of SSC, g is the number of spatial lags in model 3. Figure 4(4) starts at Dec. 18 one day ahead of other figures due to the leap year handled by satellite SeaWiFS.

Table 2—Pearson correlation coefficient (r) test between SSC at present time and its SL vector at a past time. Weeks 1, 2… 8 are in the order of the 8 weeks shown in Figure 2.

Week	7	6	5	4	3	2	1
8	0.31	0.14	0.18	0.03^*	0.09	0.15	0.18
7		0.22	0.33	0.03^*	0.26	0.3164	0.3104
6			0.29	0.15	0.27	0.26	0.16
5				0.09^*	0.1^*	0.32	0.36
4					$0.s^+$	0.18	0.19
3					S	0.07^*	0.09^+
2					S		0.39

*p-value > 0.05, no significance; $^+$ 0.01 < p-valuse < 0.05; others: p-value < 0.0001s

autocorrelation surface of SSC, as spatial lags and backward time lags increased. The correlation surface had fluctuations along g and k for each week. In particular, this fluctuation appeared significantly intense round the tsunami occurrence (Fig. 5 (3), (4), (5), (6)). Spatio-temporal correlograms of Week 1, 2 and Week 8 were very similar, their correlation surfaces were comparatively smooth, and the degree of their correlation consistently decreased as g and k increased. They can be considered the "normal" spatio-temporal correlograms.

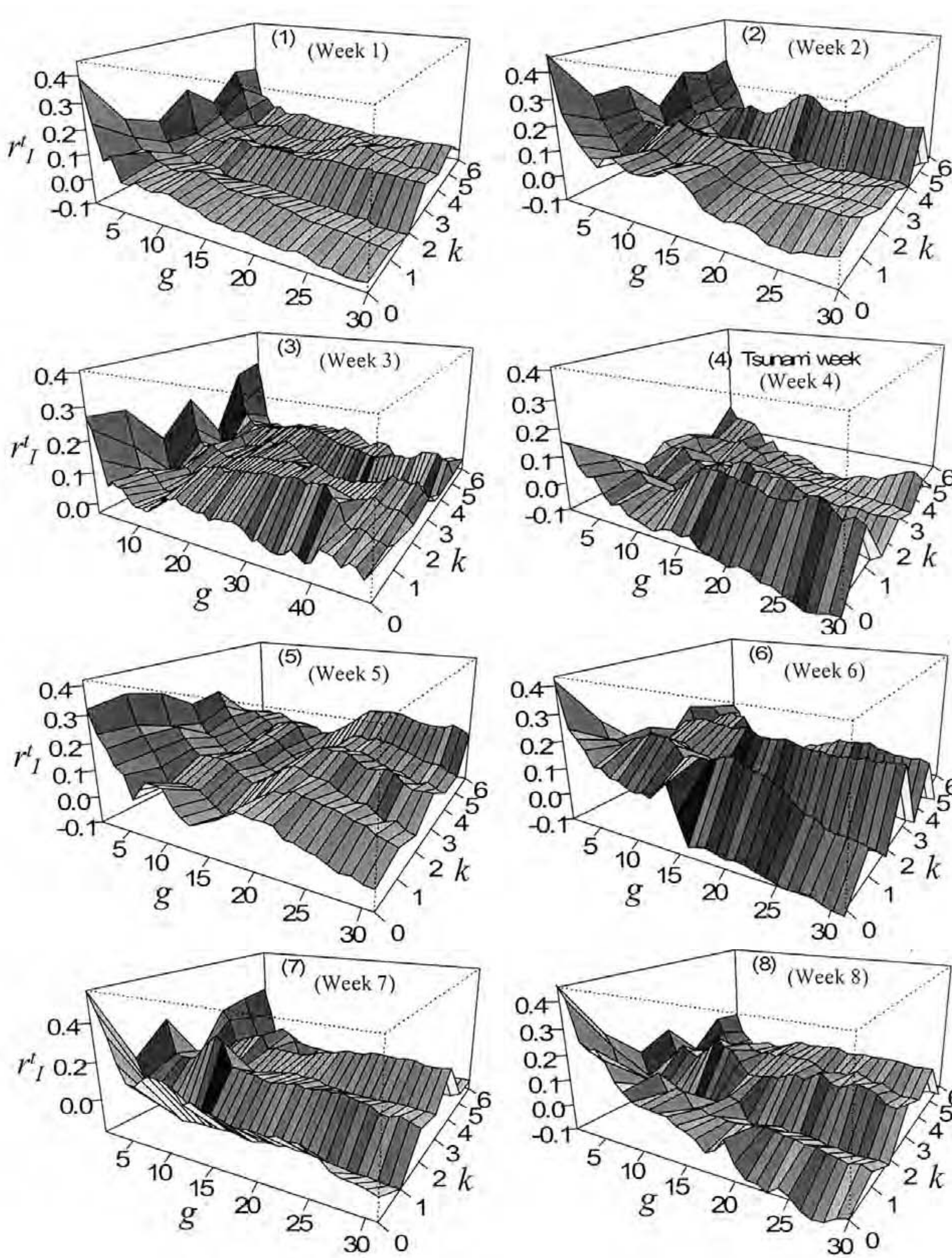

Fig. 5 —Spatio-temporal correlograms for SSC. One spatial lag is 0.5°, one backward time lag is one week. r^t_I is the spatial autocorrelation coefficient of SSC, *g* and *k* are the number of spatial lags and the number of time lags in model 4, respectively. Weeks 1, 2 … 8 are in the order of the 8 weeks shown in Figure 2.

Discussion

Changes of SSC content from the epicenter

The SSC had a drastic fluctuation in the epicenter area. Maximum of SSC content, is in Week 5 immediately after the tsunami week (Fig. 3 (1) a). The SSC in the Box Q (about 650km away from the epicenter) increased noticeably two weeks after the tsunami (Fig. 3 (1) b). SSC in Week 5 was considerably higher (about 200%) than that in the same period of Jan. 1 - 8 in 4 earlier successive years (Fig. 3 (2)). This should be related to the tsunami event. SSC is particularly affected by wind-wave resuspension, which resuspends the sediments in shallow water[11,12]. Maximum average wind speed (6.02) appeared just in Week 5 (Table 1), but it has no significant influence on SSC[19]. It should be caused mainly by the transportation of SSC, caused by the tsunami backwashing currents, that increased the spatial clustering in Week 5 and diluted subsequently by the sea currents in the epicenter area. Two weeks later, the transportation and diffusion of SSC caused by the tsunami began to affect and increase the SSC content in the sampled area of Box Q (about 650km away from the epicenter). But SSC was not influenced much in the sampled deep area about 1600 km from the epicenter area (Box S in Figure 1).

Spatial clustering level in SSC

It was obvious that the SSC had significant spatial correlation for each week (Table 1). But the degree of spatial correlation in SSC decreased significantly in the tsunami week. The degree of autocorrelation in SSC decreased gradually as spatial lags increased for all the 8 weeks (Fig. 2). The spatial lags (g) of positive correlation distance decreased considerably from 48 in Week 3 to 5 in Week 4 (tsunami week). Some high level spatial clusters of SSC were observed, along the Andhra and Tamilnadu Coasts of India and at the estuaries of some of the large rivers, several weeks after the tsunami[8,19]. In present study, our results indicated a considerable decrease of spatial clustering in Week 4, but a large increase in range immediately before the tsunami occurrence. The positive correlation distance (g) in SSC, in Week 3, was significantly longer than that in the same period of Dec. 19 - 26 in other 5 years from 2001 to 2006 (Fig. 4(4)). The decrease of spatial clustering in the tsunami week may be related to the tsunami waves that dispersed and diluted the level of spatial clustering of SSC distribution. The significant increase of spatial correlation distance in SSC distribution (Fig. 2(3), Fig. 4(4)), immediately before the tsunami event, indicated that the flow of sea water among neighboring locations (or grids) enhanced markedly. The specific reason for the anomalous enhancement of the flowing of sea water, among neighboring locations and immediately before the tsunami event, is still not clear.

Temporal correlation of SSC

A general trend of decrease in correlation was observed over time (along each row of Table 2), but this pattern was not consistent. This indicated that the spatial distribution in SSC in a past week had a positive effect on that in the present week, and the spatial variations in SSC distribution showed continuity along time. It was noticeable that, except Week 6, the spatial distribution of SSC in the tsunami week had no significant influence on that in Week 5, 7 and 8 after the tsunami (column of Week 4 in Table 2). This might suggest that the tsunami significantly disarranged the spatial distribution and the state of spatial clustering in SSC in the tsunami week.

Spatial and temporal dynamics of SSC

New spatio-temporal correlation model (4), showed that there was a general trend of decrease in the spatial autocorrelations of SSC along spatial lags and backward time lags, respectively. Correlation surface had notable fluctuations along spatial lags and time lags for each week. In particular, this fluctuation appeared largely and significantly intense round the tsunami occurrence (Figure 5 (3), (4), (5), (6)). Intense fluctuation in Week 3, immediately before the tsunami occurrence, had spatial lags of positive correlation (g) near 50, which exceeded considerably the positive correlation distance in other weeks. Spatio-temporal correlation surface is related closely to the spatial consistency along spatial lags, and to the temporal consistency along time lags in SSC distribution. Floods can enhance markedly the transfer of sediments and contaminants from the coastal zones to the sea[15]. Suspended sediments, transported by the tsunami backwashing floods, may have suddenly and considerably disrupted the temporal and spatial consistency in SSC distribution, simultaneously along time and space.

Earthquakes can induce sudden changes in the ocean-atmosphere interactions. Some studies have shown that anomalous behaviors, in the ocean-atmosphere interactions, are believed to show precursory signals of earthquakes[24,25]. Spatio-temporal variability of SSC is one of the ocean-atmosphere interaction processes (such as sea currents and wind). Accordingly, the significantly intense fluctuation of spatio-temporal correlation in SSC, immediately round the tsunami occurrence (Figure 5 (3), (4), (5), (6)), may be related closely to the tsunami event. Thus, the intense fluctuation in the correlation surface of SSC, with anomalous longer positive correlation distance in Week 3 (immediately before the tsunami event), might be a precursor of the earthquake and tsunami occurrence. SSC in coastal seas has a direct influence on pollutants to the oceans[6]. SSC is even taken as a surrogate for contaminant concentration in coastal shallow waters[14]. Accordingly, physical processes that affect SSC also affect largely the concentrations of associated contaminants[26]. The 2004 Sumatra tsunami significantly disturbed the spatio-temporal dynamics in SSC distribution. It may also have affected the spatio-temporal variability of sediment-associated contaminants.

Conclusion

SSC in the epicenter area had a drastic fluctuation, and it was significantly higher immediately after the tsunami week than that in other weeks. SSC in the epicenter area in Week 5 was about 200% higher than that in the same period of Jan. 1 - 8 in 4 earlier successive years. But SSC in a sampled deep area of the sea, about 1600 km from the epicenter, did not change much. The transportation of SSC, caused by the tsunami backwash, should be mainly responsible for the anomalous increase in SSC immediately after the tsunami week, and the sea currents diluted SSC afterwards. Two weeks later, the transportation and diffusion of SSC began to affect and increase the SSC content in the sampled area of Box Q (about 650km away from the epicenter). But this affection was not observed in a deep area of the ocean (Box S) about 1600km away from the epicenter. The effect of the tsunami on SSC decreased significantly along the distance from the epicenter to away from the epicenter.

The range and degree of spatial clustering in SSC decreased largely in the tsunami week. The tsunami waves, in the tsunami week, should have weakened and diluted the level of spatial clustering in SSC distribution. The significant increase of the spatial correlation distance in SSC distribution indicated that the flow of sea water, among neighboring locations (or grids), markedly enhanced immediately before the tsunami event.

New developed spatio-temporal correlation model (4) shows that the fluctuation, in the spatio-temporal correlation surface of SSC, appeared largely and significantly intense round the tsunami occurrence. It should suggest that the tsunami disturbed considerably the spatial and temporal dynamics in SSC distribution, simultaneously along space and time. The tsunami may also have affected the spatio-temporal variability of sediment-associated contaminants. This new developed spatio-temporal correlation model is helpful in understanding the spatio-temporal dynamics of SSC during the tsunami period.

Acknowledgements

This work was supported by research grants awarded to Dr. Tang DL: (1) National Natural Sciences Foundation of China (40576053, 40811140533, 40976091), (2) The CAS/SAFEA International Partnership Program for Creative Research Teams (KZCX2-YW-T001), and (3) Knowledge innovation program (LYQY200701) of SCS, CAS.

References:

1 Borero, J.C., Field Data and Satellite Imagery of Tsunami Effects in Banda Aceh, *Science*, 308 (2005) 1596.

2 Liu, P.L.F., Lynett, P., Fernando, H., Jaffe, B.E., Fritz, H., Higman, B., Morton, R., Goff, J. & Synolakis, C., Observations by the International Tsunami Survey Team in Sri Lanka, *Science*, 308 (2005) 1595.

3 UNEP, *After the Tsunami: Rapid Environmetal Assessment* (United Nations Environment Programme, Nairobi) (2005).

4 Dahdouh-Guebas, F. & Koedam, N., Coastal Vegetation and the Asian Tsunami, *Science*, 311 (2006) 37.

5 Tang, D.L., Zhao, H., Satyanarayana, B., Zheng, G.M., Singh, R.P. & Lv, J.H., Enhancement of Chlorophyll-a in the Northeastern Indian Ocean after the (2004) South Asian Tsunami, *Int. J. Remote Sens.*, 30 (17) (2008) 4553-4565.

6 Eisma, D., Suspended matter as a carrier for pollutants in estuaries and the sea, in: *Marine Environmental Pollution, vol. 2, Dumping and Mining*, edited by R.A. Geyer, (Elsevier Oceanographic Series 27B) (1981), pp. 281-295.

7 Nittrouer, C.A. & Kuehl, S.A., Geological significance of sediment transport and accumulation on the Amazon continental shelf, *Mar. Geol.*, 125 (1995) 175-176.

8 Yan, Z. & Tang, D.L., Changes in suspended sediments associated with 2004 Indian Ocean tsunami, *Adv. Space Res.*, 43 (2009) 89-95.

9 De Haas, H. & Eisma, D., Suspended-sediment transport in the Dollard estuary, *Neth. J. Sea Res.*, 31 (1) (1993) 37-42.

10 Ridderinkhof, H., Van der Ham, R. & Van Der Lee, W., Temporal variations in concentration and transport of suspended sediments in a channel-flat system in the Ems–Dollard estuary, *Cont. Shelf Res.*, 20 (2000) 1479-1493.

11 Powell, T.M., Cloern, J.E. & Huzzey, L.M., Spatial and temporal variability in South San Francisco Bay (U.S.A). Horizontal distributions of salinity, suspended sediments, and phytoplankton biomass and productivity, *Estuar. Coast. Shelf Sci.*, 28 (1989) 583-597.

12 Schoellhamer, D.H., Factors affecting suspended-solids concentrations in South San Francisco Bay, California, *J. Geophys. Res.*, 101 (C5) (1996) 2087-2095.

13 Ramaswamy, V., Rao, P.S., RAO, K.H., Thwin, S., Rao, N.S. & Raiker, V., Tidal influence on suspended sediment distribution and dispersal in the northern Andaman Sea and Gulf of Martaban, *Mar. Geol.*, 208 (2004) 33-42.

14 Schoellhamer, D.H., Mumley, T.E. & Leatherbarrow, J.E., Suspended sediment and sediment-associated contaminants in San Francisco Bay, *Environ. Res.*, 105 (2007) 119-131.

15 Zonta, R., Collavini, F., Zaggia, L. & Zuliani, A., The effect of floods on the transport of suspended sediments and contaminants: A case study from the estuary of the Dese River (Venice Lagoon, Italy), *Environ. Int.*, 31 (2005) 948-958.

16 Weeks, A.R. & Simpson, J.H., The measurement of suspended particulate concentrations from remotely sensed data, *Int. J. Remote Sens.*, 12 (1991) 725-737.

17 Bowers, D.G., Boudjelas, S. & Harker, G.E.L., The distribution of fine suspended sediments in the Irish Sea and its dependence on tidal stirring, *Int. J. Remote Sens.*, 19 (1998) 2789-2805.

18 Anilkumar, N., Sarma, Y.V.B. & Babu, K.N., Post-tsunami oceanographic conditions in southern Arabian Sea and Bay of Bengal, *Curr. Sci.*, 90 (3) (2006) 10.

19 Zhang, X.F., Tang, D.L., Li, Z.Z. and Zhang F.P., The effects of wind and rainfall on suspended sediment concentration related to the (2004) Indian Ocean tsunami, *Mar. Pollut. Bull.*, 58 (2009) 1367-1373.

20 Lee, S., Developing a bivariate spatial association measure: An integration of Pearson's r and Moran's *I*, *J. Geogr. Syst.*, 3 (2001) 369-385.

21 Reza, M.M. & Hamid, M., Remote sensing of suspended sediments in surface waters, using Modis images, (ISPRS 20th Congress, 35, Istanbul) (2004), pp. 1682-1750.

22 Tan, C.K., Ishizaka, J., Matsumura, S., Yusoff, F.M. & Mohamed, M.I., Seasonal variability of SeaWiFS chlorophyll-a in the Malacca Straits in relation to Asian monsoon, *Cont. Shelf Res.*, 26 (2006) 168-178.

23 Whittle, P., On the stationary processes in the plane, *Biometrika*, 41 (1954) 434-449.

24 Sousa, W.P., Disturbance in Marine Intertidal Boulder Fields: The Nonequilibrium Maintenance of Species Diversity. *Ecology*, 60 (1979) 1225-1239.

25 Hayakawa, M., Fujinawa, Y., Evison, F.F., Shapiro, V.A., Varotsos, P., Fraser-Smith, A.C., Molchanov, O.A., Pokhotelov, O.A., Enomoto, Y. & Schloessin, H.H., What is the future direction of investigation on electromagnetic phenomena related to earthquake prediction, in: *Electromagnetic Phenomena Related to Earthquake Prediction*, edited by M. Hayakawa and Y. Fujinawa, (Terra Scientific Publishing Company, Tokyo) (1994), pp. 667-677.

26 Schoellhamer, D.H., Shellenbarger, G.G., Ganju, N.K., Davis, J.A. & Mckee, L.J., Sediment dynamics drive contaminant dynamics, in: *The Pulse of the Estuary: Monitoring and Managing Contamination in the San Francisco Estuary*, (San Francisco Estuary Institute, Oakland, CA) (2003), pp. 21-26.